Single laser pulse induced magnetization switching in in-plane magnetized GdCo alloys

Jun-Xiao Lin, Michel Hehn, Thomas Hauet, Yi Peng, Junta Igarashi, Yann Le Guen, Quentin Remy, Jon Gorchon, Gregory Malinowski, Stéphane Mangin, et al.

Letter

Single laser pulse induced magnetization switching in in-plane magnetized GdCo alloys

Jun-Xiao Lin,[1] Michel Hehn,[1,2] Thomas Hauet,[1] Yi Peng,[1] Junta Igarashi,[1] Yann Le Guen,[1] Quentin Remy,[3] Jon Gorchon,[1] Gregory Malinowski,[1] Stéphane Mangin,[1,2,*] and Julius Hohlfeld[1]

[1]*Université de Lorraine, CNRS, Institut Jean Lamour, F-54000 Nancy, France*

[2]*Center for Science and Innovation in Spintronics (CSIS), Tohoku University, Sendai 980-8577, Japan*

[3]*Department of Physics, Freie Universität Berlin, 14195 Berlin, Germany*

(Received 21 August 2023; accepted 27 November 2023; published 21 December 2023)

The discovery of all-optical ultrafast deterministic magnetization switching has opened up new possibilities for manipulating magnetization in devices using femtosecond laser pulses. Previous studies on single pulse all-optical helicity-independent switching (AO-HIS) have mainly focused on perpendicularly magnetized thin films. This work presents a comprehensive study on AO-HIS for in-plane magnetized Gd_xCo_{100-x} thin films. Deterministic single femtosecond laser pulse toggle magnetization switching is demonstrated in a wider concentration range ($x = 10-25\%$) compared to the perpendicularly magnetized counterparts with GdCo thicknesses up to 30 nm. The switching time strongly depends on the Gd_xCo_{100-x} concentration, with lower Gd concentration exhibiting shorter switching times (less than 500 fs). Our findings in this geometry provide insights into the underlying mechanisms governing single pulse AO-HIS, which challenge existing theoretical predictions. Moreover, in-plane magnetized Gd_xCo_{100-x} thin films offer extended potential for optospintronic applications compared to their perpendicular magnetized counterparts.

DOI: 10.1103/PhysRevB.108.L220403

Introduction. The advancement of magnetic data storage, memories, and logic devices requires a fast and energy-efficient method for manipulating magnetization in thin magnetic media and heterostructures like magnetic tunnel junctions and spin valves. While significant progress has been made in current-induced magnetic switching over the past 25 years, the typical time required for this process is still orders of magnitude slower than optically induced magnetization manipulation [1–4]. In 2012, Ostler *et al.* achieved field-free ultrafast magnetization reversal by irradiating a femtosecond laser pulse onto a ferrimagnetic GdFeCo alloy [5]. This breakthrough paved the way for all-optical helicity-independent switching (AO-HIS), although its underlying mechanism remains a topic of debate [6–12]. The reversal mechanism is primarily attributed to a pure ultrafast thermal effect on magnetization, enabled by ultrafast demagnetization and subsequent angular momentum exchange between rare-earth and transition-metal sublattices on subpicosecond and picosecond time scales [5,10–17]. This enables reliable writing of magnetic bits at GHz frequencies [18,19].

AO-HIS has been mainly reported in perpendicularly magnetized Gd-based alloys or multilayers [5–26]. GdFeCo and GdCo alloys have been extensively studied. They are ferrimagnetic alloys for which the magnetization of the Gd sublattice (M_{Gd}) is exchange-coupled antiferromagnetically to the magnetization of the transition metal (Fe, Co) sublattice (M_{Co}). The resulting magnetization depends on the alloy concentration and temperature. Due to the antiferromagnetic coupling of the sublattices, the net magnetization is zero at the so-called compensation composition (x_{comp}) which depends on temperature. It has been shown that AO-HIS, measured at room temperature, occurs in $Gd_x(FeCo)_{100-x}$ only when x is close to x_{comp} (at room temperature) within a few percent [10,20–23]. Theoretical models tend to confirm that only alloys with a concentration close to the x_{comp} could exhibit AO-HIS [22]. In 2015, Atxitia *et al.* used an atomistic stochastic Landau-Lifshitz-Gilbert equation for semiclassical spins, described by a Heisenberg Hamiltonian, to model AO-HIS in rare earth–transition metal ferrimagnetic alloys and concluded that a low net magnetization is an important ingredient for an energy-efficient AO-HIS [25]. The same conclusions were drawn a few years later by Jakobs *et al.* [11] by using an atomistic model and the so-called two-temperature model, and by Davies *et al.* [23] who used a phenomenological framework showing theoretical agreement with experimental results.

With the exception of a single experimental study conducted on in-plane magnetized $Gd_{25}(FeCo)_{75}$ microstructures with a specific Gd concentration [5], all previous experimental results in this field have been obtained using samples exhibiting strong perpendicular magnetic anisotropy (PMA) [5–23,25,26]. Undeniably, PMA samples offer technical advantages for performing experiments, as the pump and probe beams can be directed perpendicular to the sample's surface. However, these samples may face challenges related to the stabilization of maze domain structures, which can limit the observation of AO-HIS only when the net magnetization and the thickness of the layers are low [21,24–26]. In cases where the magnetization is high and the alloy concentration is far from x_{comp}, the magnetic configuration tends to break into domains after laser excitation to minimize dipolar (demagnetization)

*Corresponding author: stephane.mangin@univ-lorraine.fr

energy [26,27]. Consequently, we can question whether the theoretical notion that a concentration close to compensation (i.e., low magnetization) is an intrinsic and mandatory requirement for achieving AO-HIS or whether it is an extrinsic effect driven by domain structure stabilization. In contrast to PMA systems, in-plane magnetized thin films are not expected to experience a strong dipolar field that induces a multidomain state. Therefore, studying these films can help addressing uncertainties regarding intrinsic and extrinsic effects.

This Letter presents a comprehensive investigation into the manipulation of magnetization using a single femtosecond laser pulse in in-plane magnetized Gd_xCo_{100-x} thin films. Unlike perpendicularly magnetized $Gd_x(FeCo)_{100-x}$ films, we were able to successfully demonstrate AO-HIS over a wide range of concentrations ($5\% < x < 30\%$) and thicknesses (5–30 nm). This observation challenges existing theoretical predictions, which suggest a narrow concentration range around compensation for AO-HIS. By analyzing the laser-induced effects, we identified three distinct threshold fluences that play a crucial role in observing AO-HIS: the fluence required for magnetization switching ($F_{\mathrm{Sw}}^{\mathrm{th}}$), the fluence for demagnetization ($F_{\mathrm{Dem}}^{\mathrm{th}}$) for which the multidomain patterns are created due to excessive heating of the sample, and the fluence that causes irreversible changes or damage to the magnetic properties ($F_{\mathrm{Dam}}^{\mathrm{th}}$). $F_{\mathrm{Sw}}^{\mathrm{th}}$ exhibited a minimum at compensation, while $F_{\mathrm{Dem}}^{\mathrm{th}}$ increased with the sample's Curie temperature. The magnetization dynamics during the reversal process resembled those observed in perpendicularly magnetized films, with the fastest switching occurring for the lowest Gd concentration.

Methods:

Sample preparations. Glass/Ta (3 nm)/Gd_xCo_{100-x} (t nm)/Cu (1 nm)/Pt (3 nm) samples with different x and t values were prepared through magnetron cosputtering with elemental targets processed under an argon gas pressure of approximately 10^{-3} mbar. Multilayered typical structures were deposited onto $15 \times 10-$mm glass substrates. The Ta layer at the bottom plays a crucial role in enhancing the adhesion of the structure to the substrate, while the upper Pt serves as a widely employed protective layer against sample oxidation. The GdCo alloys were fabricated using two separate targets: a Gd and a Co. While depositing the GdCo onto the glass substrate at room temperature, we deliberately ensured the layer deposition was made in the stray field of the gun of the magnetron by sweeping the sample over both targets: this produces a well-defined in-plane anisotropy in Gd_xCo_{100-x} (t nm), as shown in Fig. S9(b) of the Supplemental Material [28]. Furthermore, to avoid any reorientation of magnetization out of the plane, especially in the vicinity of the compensation point due to the reduction of the demagnetizing field, Ta and Cu interfaces were used instead of Pt. This choice was made due to the well-known strong surface anisotropy exhibited by Pt when in contact with Co. In samples for the thickness-dependent all-optical helicity-independent switching (AO-HIS) experiments, the Gd_xCo_{100-x} (t nm) concentration is fixed at $x = 25\%$ while t varies from 5 to 35 nm with an interval of 5 nm.

Characterizations. Static single pulse and time-resolved measurements were performed in a longitudinal magneto-optic Kerr effect (MOKE) configuration [Fig. 1(a)]. Samples

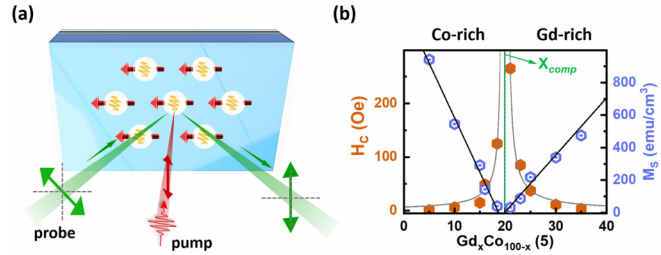

FIG. 1. (a) Schematic of the static single laser pulse and time-resolved measurements based on longitudinal magneto-optic Kerr effect (MOKE). The linearly polarized pump laser pulse (wavelength = 800 nm, pulse length = 150 fs) is shined perpendicular to the film plane, whereas the linearly p-polarized probe beam (wavelength = 515 nm) angle of incidence is 45°. The reflected optical probe beam is sent to a camera for MOKE images. The sample is initialized using an external in-plane magnetic field before pumping the laser pulse. The red three-dimensional arrows represent the Co magnetic moments. Experiments were carried out at room temperature. (b) Variation of the coercive field H_C (solid orange symbols) and the saturation magnetization M_S (open violet symbols) as a function of Gd content x in glass/Ta (3 nm)/Gd_xCo_{100-x} (5 nm)/Cu (1 nm)/Pt (3 nm).

were studied in an optical setup integrated with a dipole electromagnet, allowing for a variable field (0–0.3 T) operation along the sample plane. The linearly polarized pump pulse with a spot size diameter of $\sim$ 120 μm was normal incident to the sample surface. On the other hand, the linearly p-polarized probe beam with low energy impinged on the sample at an incidence angle of 45° to obtain the MOKE images using a complementary metal oxide semiconductor camera. The samples are thin films deposited on the glass substrates. We define the side where the film is deposited as the top side and the uncovered side of the substrate as the back side. In this work, both laser pump and probe beams were shined on the top side. The wavelength of the pump pulse was fixed at 800 nm, and the one for the probe beam was set at 515 nm, which mainly reflects the magnetic signals of the Co sublattice of GdCo alloys. One crucial parameter for all the AO-HIS measurements: the laser pulse length was fixed at 150 fs. All measurements were performed at ambient temperature.

For the static single pulse AO-HIS measurements, the external in-plane magnetic field [oriented parallel to the substrate and along the in-plane easy axis, as indicated in Fig. S9(c)] with a strength larger than the sample coercivity was first applied to initialize the sample [28]. Thereby all the moments in the alloy were aligned in the direction of the in-plane easy axis after turning off the field. Subsequently, the samples were irradiated by different numbers of laser pump pulses without any external magnetic field to perform the static single pulse AO-HIS measurements. The repetition rate of the laser pump pulse was set to 100 kHz for all static single pulse AO-HIS measurements.

On the other hand, for the time-resolved MOKE imaging measurements, an in-plane magnetic field with a strength around the sample coercivity was always applied along the initial in-plane easy axis direction of magnetization to initialize the sample before each pump pulse. The field value varies from one sample to another due to the different coercivities of

all investigated samples. We used the MOKE imaging configuration to perform the dynamic measurements, however these may include some artificial optical signals originating from a substrate or environment. To remove those signals, we took the intensity difference for opposite magnetization directions at negative time delay to normalize the presented data, as described in a previous study [29]. Here, the delay time zero was determined by the time where the derivative of the magnetization dynamics trace is maximal. We employed a repetition rate of 100 kHz for both the pump and probe beams for samples with Gd concentrations of $x = 16\%$, 18.4%, 21%, and 23%. However, for samples with Gd concentrations of $x = 10\%$ and 25%, the repetition rate was reduced to 10 kHz, as the threshold for causing permanent damage to the samples varies from one sample to another, and so does their capacity to endure a specific temperature within a given time frame. The saturation magnetization and coercivity in Fig. 1(b) and the magnetization versus magnetic field curves in Fig. S2 [28] were studied using a superconducting quantum interference device.

Experimental results:

Magnetic properties of in-plane magnetized Gd_xCo_{100-x} *thin films.* Gd_xCo_{100-x} ferrimagnetic thin films consisting of Glass/Ta (3 nm)/Gd_xCo_{100-x} (t nm)/Cu (1 nm)/Pt (3 nm) were prepared with a wide range of Gd concentration x, varying from 5% to 35% and a wide range of Gd_xCo_{100-x} thickness t, varied from 5 to 35 nm. In all cases, the Gd_xCo_{100-x} interfaces were designed to keep an easy uniaxial anisotropy axis in-plane for any x and t values. Figure 1(b) summarizes the evolution of the magnetization and coercivities of the sample as a function of the concentration for $t = 5$ nm. As expected, the coercivity diverges, and the net magnetization reaches zero around $x = 20\%$, corresponding to the compensation composition (x_{comp}) at room temperature. M_{Co} is dominant over M_{Gd} when $x < 20\%$, while M_{Gd} becomes dominant as $x > 20\%$. As shown in Supplemental Material 1, all hysteresis loops measured with an in-plane field have a remanence close to 1, revealing the existence of a well-defined in-plane magnetic anisotropy axis in all Gd_xCo_{100-x} films [28]. This is also confirmed by the angle-dependent remanence measurements shown in Supplemental Material 9 [28]. Moreover, the out-of-plane magnetic field-dependent saturation magnetization measurements for all the samples are provided in Supplemental Material 2, indicating that the hard axis is mainly perpendicular to the sample surface [28]. The evolution of Kerr microscope images as a function of an in-plane magnetic field applied along the easy axis shows that the domain size and the domain growth by domain wall motion are similar for all GdCo concentrations (Supplemental Material 3 [28]).

Concentration-dependent single pulse all-optical helicity-independent switching for in-plane magnetized Gd_xCo_{100-x} *alloys.* A sketch of the experimental setup is shown in Fig. 1(a). It is based on a standard longitudinal magneto-optic Kerr effect (MOKE) configuration that allows tracking the in-plane magnetization changes after shining linearly polarized femtosecond laser pulses. One important parameter, the pulse length, has been fixed to 150 fs, and further details are given in *Characterizations*. Figure 2(a) demonstrates that for a $Gd_{15}Co_{85}$ in-plane magnetized thin film, it is possible to observe a deterministic single pulse all-optical helicity-independent switching (AO-HIS), independent of the initial direction of magnetization. First, two domains with opposite directions along the in-plane easy axis were created using an in-plane external magnetic field; then, laser pulses were shined at three different positions under zero applied field. As a result, one can clearly observe that a full magnetization switching is observed for the two initial magnetization directions. Moreover, we confirmed that a full switching is indeed observed since the contrast variations between the magnetic field-induced and the laser-induced switching are the same.

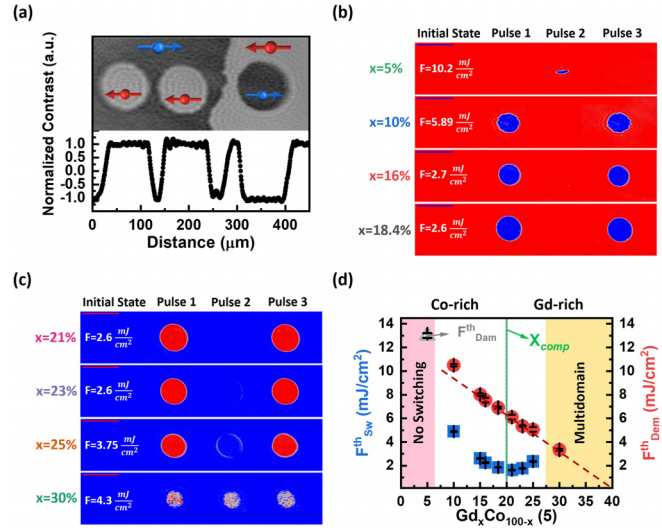

FIG. 2. AO-HIS in 5-nm-thick Gd_xCo_{100-x} alloys (a) Kerr images and normalized contrast cross section after three single laser shots inducing AO-HIS for a $Gd_{15}Co_{85}$ thin film starting from a two-domain magnetic state of opposite directions along the easy axis. The blue and red arrows indicate the Co sublattice's magnetization direction. Magneto-optic contrast obtained after a single 150-fs laser pump pulse on various in-plane magnetized Gd_xCo_{100-x} alloys: (b) for Co-dominant samples and (c) for Gd-dominant samples. For each measurement, the laser pulses were shined at the same position. A scale bar of 100 μm is presented. (d) The switching threshold (F^{th}_{Sw}) and demagnetization threshold (F^{th}_{Dem}) fluences as a function of Gd concentrations. Note that the grey open triangle indicates the threshold to permanently damage the sample (F^{th}_{Dam}), and the red dashed line guides the eye for the F^{th}_{Dem}.

The laser-induced magnetization switching obtained for various Gd_xCo_{100-x} concentrations is shown in Figs. 2(b) and 2(c). They present the MOKE images obtained after shining 0, 1, 2, and 3 pulses at the same position for a series of 5-nm Gd_xCo_{100-x} alloy samples. AO-HIS is demonstrated for x ranging 10–25%. In this case, a fully reversed domain appears after the first pulse, completely vanishes after the second pulse, and fully reappears after the third one, indicating a perfect toggle-switching behavior. In addition, a multidomain state is formed in the center region of the spot when the laser fluence is large enough (Supplemental Material 4 [28]). Perfect toggle switching for in-plane magnetized GdCo films is observed even after 1000 pulses, as shown in Supplemental Material 5, demonstrating the endurance of AO-HIS in such films potentially for technological applications [28]. To make sure that dipolar fields are not affecting the switching, AO-HIS has been demonstrated when shining laser

pulses on the boundary between two domains, as shown in Supplemental Material 6 [28]. The effect of single laser pulses was also studied for samples with excessive content of Co (i.e., $x = 5\%$) and Gd (i.e., $x = 30\%$). For $x = 5\%$, neither a typical round-shaped switching pattern nor a multidomain state was observed before the degradation of the sample, as shown in Supplemental Material 7 [28]. For $x = 30\%$, either no switching or a multidomain state was obtained, as shown in Supplemental Material 8 [28]. Nevertheless, as shown for heat-assisted magnetic recording, those disordered patterns can be removed, and magnetization can be reversed by applying a tiny external field along the direction opposite to the initial magnetization direction [30,31]. Supplemental Material 9 compares the effect of light when the sample is saturated along the easy and in-plane hard axes for $Gd_{15}Co_{85}$ [28]. Along the easy axis, as reported earlier, full switching is demonstrated. However, when the sample is first saturated along the in-plane hard axis, and then the field is removed, the remanent state is multidomain; consequently, no single-domain all-optical switching could be observed. On the other hand, partial light-induced switching is clearly demonstrated.

To summarize AO-HIS in GdCo in-plane magnetized alloy samples, Fig. 2(d) shows the threshold fluence needed to observe switching ($F_{\mathrm{Sw}}^{\mathrm{th}}$) and threshold fluence needed to demagnetize the sample [$F_{\mathrm{Dem}}^{\mathrm{th}}$; i.e., when the multidomain state is formed in the irradiation area in the case of too high pump pulse fluence, as shown in Fig. S4(c)] as a function of the Gd concentrations [28]. This diagram clearly demonstrates that the window of Gd concentration (Δx) exhibiting the AO-HIS is much larger for in-plane magnetized GdCo alloys ($\Delta x \sim 20\%$) compared to perpendicular magnetic anisotropy (PMA) GdFeCo alloys ($\Delta x \sim 5\%$) [10,20,21] and pure PMA GdCo alloys ($\Delta x \sim 9\%$) [22,32]. The diagram also shows that a minimum in $F_{\mathrm{Sw}}^{\mathrm{th}}$ can be observed close to the x_{comp}, whereas $F_{\mathrm{Dem}}^{\mathrm{th}}$ decreases monotonically with increasing Gd concentration, following a similar trend to that of the Curie temperature (T_{C}) (Supplemental Material 10 [28]). Note that a third threshold fluence ($F_{\mathrm{Dam}}^{\mathrm{th}}$) can be defined as the fluence threshold which damages the sample such that it cannot recover its initial magnetic state. The reason why no AO-HIS is observed for $x = 5\%$ and $x = 30\%$ would then come from two different reasons. As we will discuss later, no AO-HIS is observed because $F_{\mathrm{Sw}}^{\mathrm{th}} > F_{\mathrm{Dam}}^{\mathrm{th}}$ for $x = 5\%$, and because $F_{\mathrm{Sw}}^{\mathrm{th}} > F_{\mathrm{Dem}}^{\mathrm{th}}$ for $x = 30\%$. For the PMA $Gd_x(FeCo)_{100-x}$ alloys, it has been shown that the laser pump energy required to produce AO-HIS is minimum around x_{comp} [20–22,33], which is in agreement with in-plane magnetized GdCo alloys. This hints that in-plane magnetized GdCo alloys should share the same switching mechanism as perpendicularly magnetized GdCo alloys.

Thickness-dependent single pulse all-optical helicity-independent switching for in-plane magnetized GdCo alloys. After investigating the influence of the GdCo alloy concentration on AO-HIS, we now study its thickness dependence. For this study, we fixed the arbitrary Gd concentration x to 25% ($Gd_{25}Co_{75}$). Normalized longitudinal MOKE hysteresis loops for various thicknesses are shown in Supplemental Material 11 [28]. Square hysteresis loops are observed along the in-plane easy axis for all thicknesses ranging 5–35 nm, demonstrating a strong in-plane anisotropy easy axis for all

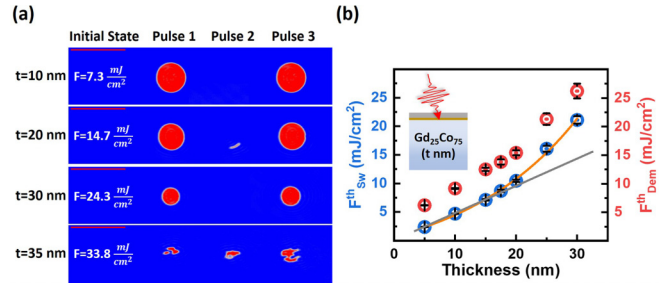

FIG. 3. (a) Static MOKE images obtained after single laser pump pulse irradiation for different thicknesses (t) of the in-plane magnetized $Gd_{25}Co_{75}$ thin film. The scale bar is 100 μm long. (b) Dependence of $F_{\mathrm{Sw}}^{\mathrm{th}}$ and $F_{\mathrm{Dem}}^{\mathrm{th}}$ as a function of thickness. The orange line is obtained from a fitting using an exponential function. The linear grey line is a guide for the eye.

thicknesses. Figure 3(a) demonstrates deterministic toggling AO-HIS for thickness (t) $\leqslant 30$ nm. $F_{\mathrm{Sw}}^{\mathrm{th}}$ and $F_{\mathrm{Dem}}^{\mathrm{th}}$, as a function of the $Gd_{25}Co_{75}$ thickness, are shown in Fig. 3(b).

Both $F_{\mathrm{Sw}}^{\mathrm{th}}$ and $F_{\mathrm{Dem}}^{\mathrm{th}}$ exhibit a similar trend: there is an exponential increase which diverges around a value close to the typical light penetration depth (approximately 20 nm in our case). As shown in Supplemental Material 12, where we observe that for thin GdCo layers, the absorbed energy profile within the GdCo layer shows a relatively weak dependence on depth, implying a uniform demagnetization throughout the entire layer [28]. In general, switching and demagnetization depend on the absorbed energy density in GdCo layer and, consequently, on temperature. The fact that the two fluences tend to diverge with the GdCo thickness implies that the demagnetization can no longer be considered uniform. Indeed, the depth-dependent absorption profiles shown in Supplemental Material 12 obtained using the transfer matrix method reflect the heat absorption at different film depths [28,34,35]. The obtained absorption gradient for the thicker films implies that the laser pump pulse heats the system inhomogeneously, indicating that the front part of the sample (facing the laser pump pulse) absorbs more laser energy than the further part of the magnetic layer. If the entire GdCo layer needs to reach a certain temperature before switching, the laser fluence will then increase and tend to diverge as the sample thickness increases. We can then speculate that the speckled magnetic domain observed for $Gd_{25}Co_{75}$ with a thickness of $t = 35$ nm could be understood by the fact that the front part of the sample absorbs enough energy to demagnetize this area, whereas the back part does not absorb enough energy to switch, resulting in a mazelike domain structure.

Time-resolved magneto-optic Kerr measurements. After investigating the effect of a single femtosecond laser pulse using Kerr images taken several seconds after the excitation, we are now probing the fast magnetization dynamics of 5-nm Gd_xCo_{100-x} samples using longitudinal time-resolved MOKE (TR-MOKE). TR-MOKE measurements were performed for samples showing toggle-switching behavior. Since the magnetization dynamics depend strongly on the laser fluence, in an effort to normalize the laser fluence, for each concentration, we used a laser fluence 1.2 times larger than the previously determined threshold fluence $F_{\mathrm{Sw}}^{\mathrm{th}}$. As observed

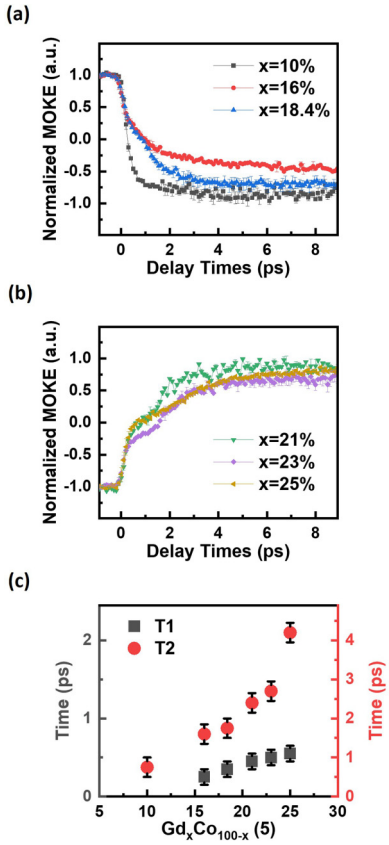

FIG. 4. Normalized longitudinal MOKE signal as a function of time for Gd_xCo_{100-x} (5 nm) for (a) Co-dominant alloys ($x = 10\%$, 16%, and 18.4%) and (b) Gd-dominant alloys GdCo ($x = 21\%$, 23%, and 25%). The measurements were obtained with an external magnetic field along the in-plane initial easy-axis direction and for fluences 1.2 times larger than the switching threshold fluence (F_{Sw}^{th}). (c) Evolution of two characteristic times (T1 and T2) of the switching as a function of the Gd_xCo_{100-x} concentration.

in Figs. 4(a) and 4(b), all curves showed similar features: a fast initial drop followed by a slower decrease and a saturation toward the opposite magnetic state. This type of feature has already been seen for the AO-HIS in the single-layer PMA GdFeCo alloys demonstrated by different research groups [6,8,11,36]. This indicates, as expected at short time scales, that the AO-HIS effect is independent of the magnetic anisotropy and should originate from a purely ultrafast thermal effect [5,6,10,11,21,22]. To qualitatively describe the dynamics traces, we defined two characteristic times: T1 corresponding to the time at the end of the first fast drop and T2 to the time corresponding to the end of the slower decrease, as shown in Supplemental Material 13 [28]. In Fig. 4(c), T1 and T2 are plotted as a function of the Gd concentration. Those measurements show that the magnetization dynamics of Co slow down with increasing Gd concentration.

Discussion. The obtained results provide clear evidence of *single pulse*, *ultrafast* all-optical helicity-independent switching (AO-HIS) in in-plane magnetized GdCo alloys. Notably, this AO-HIS phenomenon is observed over a significantly larger concentration and thickness range compared to previous experimental observations in perpendicularly magnetized systems [10,11,20,21,32,37] and theoretical predictions [10,22,23]. The extended concentration range can be attributed to the absence of a stabilized multidomain state due to dipolar fields (stray fields or demagnetization fields) far from magnetization compensation composition (x_{comp}). In perpendicularly magnetized samples, the generation of a multidomain state by dipolar fields requires the definition of a threshold fluence, denoted as F_{Multi}^{th} [26]. Zhang *et al.* demonstrated that a criterion for observing AO-HIS is that F_{Sw}^{th} (the fluence needed for magnetization switching) is less than F_{Multi}^{th}. Otherwise, the switching process is overshadowed by the formation of the multidomain state, which occurs at a longer time scale [38]. As dipolar fields increase with sample magnetization and thickness, F_{Multi}^{th} decreases when moving away from x_{comp} and for thicker samples.

Because F_{Multi}^{th} does not need to be considered in the in-plane magnets, the observation of AO-HIS is not limited to low-thickness or low-magnetization alloys (close to compensation in the case of ferrimagnetic alloys). Accordingly, the critical criteria become $F_{Sw}^{th} < F_{Dam}^{th}$ and $F_{Sw}^{th} < F_{Dem}^{th}$. It is fair to assume that F_{Dam}^{th} does not depend on the Gd concentration, whereas F_{Dem}^{th} decreases with Gd concentration as a consequence of the decrease of Curie temperature (T_C) [39]. The latter is clearly observed in Fig. 2(d), where F_{Dem}^{th} decreases almost linearly with increasing concentration of Gd. If we extrapolate the evolution of F_{Dem}^{th} as a function of Gd concentration, $F_{Dem}^{th} = 0$ can be reached for $x = 40\%$, the concentration at which the T_C approaches 300 K [39,40]. For $x = 30\%$ (the highest Gd concentration in this work), the AO-HIS cannot be seen because of $F_{Sw}^{th} > F_{Dem}^{th}$. On the other hand, as detailed in the work of Zhang *et al.*, F_{Sw}^{th} depends both on the alloy's T_C and the amount of angular momentum generated [26]. In our work, for $x = 5\%$ (lowest Gd concentration in this work), the AO-HIS cannot be observed due to the fact that $F_{Sw}^{th} > F_{Dam}^{th}$. Because of the high T_C value of the alloy for low Gd concentration, a laser fluence larger than F_{Dam}^{th} would be needed to switch the magnetization. Furthermore, a minimum F_{Sw}^{th} appears close to x_{comp} in our study, as observed in perpendicularly magnetized GdFeCo alloys [11,20–22,25]. This is in accord with Barker *et al.* who suggested that a nonequilibrium energy transfer between the ferromagnetic- and antiferromagneticlike magnon branches is maximized near x_{comp}, resulting in a minimum F_{Sw}^{th} around x_{comp} [33].

Finally, regarding dynamics, the fastest switching is obtained for low Gd concentration and tends to increase as the Gd concentration increases, as shown in Fig. 4(c). We confirm here that the Co spin-lattice coupling is an efficient channel for angular momentum dissipation in ferrimagnetic alloys [41]. Indeed, it has been demonstrated that for GdCo alloy, the angular momentum dissipation into the lattice for Gd is less than for Co [6,41]. Adding Gd leads to changes in the speed and amplitude of both sublattices' demagnetization [22,42]. As confirmed experimentally in previous works, when ultrafast demagnetization occurs, the angular momentum will either dissipate locally into the lattice or be transferred as a spin current [4,29,41–46]. Therefore, the more Gd is introduced, the fewer dissipation channels are available at a short time scale, resulting in the slowdown of the overall magnetization dynamics. Time-resolved magneto-optic Kerr effect mea-

surements reveal two distinct relaxation times, T1 and T2, which both increase with Gd concentration (slower dynamics with more Gd), as shown in Fig. 4(c) and Supplemental Material 13 [28]. However, we cannot highlight the underlying physical mechanisms behind these time-dependent behaviors at this stage. The utilization of advanced light-source techniques [47], offering time-dependent, element-specific, and nanoscale spatially resolved capabilities, could facilitate our comprehension of the influence of Gd concentration on GdCo dynamics.

Conclusion. In conclusion, our systematic study has successfully demonstrated deterministic all-optical helicity-independent switching (AO-HIS) using a femtosecond laser pulse for in-plane magnetized Gd_xCo_{100-x} thin films at room temperature. The observation of ultrafast switching across a wide concentration range, in contrast to perpendicularly magnetized counterparts, can be attributed to the absence of perpendicular demagnetization fields which tend to break magnetization into domains. These findings challenge the notion that compensation composition and temperature are necessary to ensure AO-HIS. However, it is crucial to create conditions for which the switching fluence threshold is lower than the thresholds leading to sample damage and demagnetization in order to observe the desired switching behavior. Additionally, our results indicate that switching can be achieved in relatively thick films, depending on the demagnetization process, providing valuable insights for future stack engineering and optimization of AO-HIS. Furthermore, the magnetization dynamics observed during the reversal of in-plane magnetized GdCo alloys are similar to those observed in perpendicularly magnetized counterparts. Notably, the demagnetization speed and subsequent switching slow down with increasing Gd concentration. These experimental findings give insights into the magnetization reversal of Gd-based materials, which hold significant implications for the development of future ultrafast spintronic memory devices.

Acknowledgments. The authors thank E. Fullerton and B. Koopmans for the fruitful discussion. This work was supported by the French National Research Agency (ANR) through the France 2030 government grants EMCOM (Grant No. ANR-22-PEEL-0009), Grant No. ANR-20-CE09-0013 UFO, Grant No. ANR-20-CE24-0003 SPOTZ, the interdisciplinary project LUE "MAT-PULSE," reference ANR-15-IDEX-04-LUE, the Carnot ICEEL for the project "CAPMAT" and FASTNESS, the Région Grand Est, the Metropole Grand Nancy for the Chaire PLUS, the "FEDERFSE Lorraine et Massif Vosges 2014–2020" for the project PLUS and IOMA, a European Union Program, the European Union's Horizon 2020 research and innovation program COMRAD under the Marie Skłodowska-Curie Grant Agreement No. 861300, the ANR project. J.-X.L. has received funding from the European Union's Horizon 2020 research and innovation programme under the Marie Skłodowska-Curie Grant Agreement No. 861300. This Letter was based upon work from COST Action CA17123 MAGNETOFON, supported by COST (European Cooperation in Science and Technology).

[1] A. Kirilyuk, A. V. Kimel, and T. Rasing, Ultrafast optical manipulation of magnetic order, Rev. Mod. Phys. **82**, 2731 (2010).

[2] D. Sander, S. O. Valenzuela, D. Makarov, C. H. Marrows, E. E. Fullerton, P. Fischer, J. McCord, P. Vavassori, S. Mangin, P. Pirro, B. Hillebrands, A. D. Kent, T. Jungwirth, O. Gutfleisch, C. G. Kim, and A. Berger, The 2017 magnetism roadmap, J. Phys. D: Appl. Phys. **50**, 363001 (2017).

[3] B. Dieny, I. L. Prejbeanu, K. Garello, P. Gambardella, P. Freitas, R. Lehndorff, W. Raberg, U. Ebels, S. O. Demokritov, J. Akerman, A. Deac, P. Pirro, C. Adelmann, A. Anane, A. V. Chumak, A. Hirohata, S. Mangin, S. O. Valenzuela, M. Cengiz Onbaşlı, M. d'Aquino *et al.*, Opportunities and challenges for spintronics in the microelectronics industry, Nat. Electron. **3**, 446 (2020).

[4] J. Igarashi, W. Zhang, Q. Remy, E. Díaz, J.-X. Lin, J. Hohlfeld, M. Hehn, S. Mangin, J. Gorchon, and G. Malinowski, Optically induced ultrafast magnetization switching in ferromagnetic spin valves, Nat. Mater. **22**, 725 (2023).

[5] T. A. Ostler, J. Barker, R. F. L. Evans, R. W. Chantrell, U. Atxitia, O. Chubykalo-Fesenko, S. El Moussaoui, L. Le Guyader, E. Mengotti, L. J. Heyderman, F. Nolting, A. Tsukamoto, A. Itoh, D. Afanasiev, B. A. Ivanov, A. M. Kalashnikova, K. Vahaplar, J. Mentink, A. Kirilyuk, T. Rasing, and A. V. Kimel, Ultrafast heating as a sufficient stimulus for magnetization reversal in a ferrimagnet, Nat. Commun. **3**, 666 (2012).

[6] I. Radu, K. Vahaplar, C. Stamm, T. Kachel, N. Pontius, H. A. Dürr, T. A. Ostler, J. Barker, R. F. L. Evans, R. W. Chantrell, A. Tsukamoto, A. Itoh, A. Kirilyuk, T. Rasing, and A. V. Kimel, Transient ferromagnetic-like state mediating ultrafast reversal of antiferromagnetically coupled spins, Nature (London) **472**, 205 (2011).

[7] T. A. Ostler, R. F. L. Evans, R. W. Chantrell, U. Atxitia, O. Chubykalo-Fesenko, I. Radu, R. Abrudan, F. Radu, A. Tsukamoto, A. Itoh, A. Kirilyuk, T. Rasing, and A. V. Kimel, Crystallographically amorphous ferrimagnetic alloys: Comparing a localized atomistic spin model with experiments, Phys. Rev. B **84**, 024407 (2011).

[8] J. Gorchon, R. B. Wilson, Y. Yang, A. Pattabi, J. Y. Chen, L. He, J. P. Wang, M. Li, and J. Bokor, Role of electron and phonon temperatures in the helicity-independent all-optical switching of GdFeCo, Phys. Rev. B **94**, 184406 (2016).

[9] A. El-Ghazaly, B. Tran, A. Ceballos, C.-H. Lambert, A. Pattabi, S. Salahuddin, F. Hellman, and J. Bokor, Ultrafast magnetization switching in nanoscale magnetic dots, Appl. Phys. Lett. **114**, 232407 (2019).

[10] C. S. Davies, T. Janssen, J. H. Mentink, A. Tsukamoto, A. V. Kimel, A. F. G. van der Meer, A. Stupakiewicz, and A. Kirilyuk, Pathways for single-shot all-optical switching of magnetization in ferrimagnets, Phys. Rev. Appl. **13**, 024064 (2020).

[11] F. Jakobs, T. A. Ostler, C.-H. Lambert, Y. Yang, S. Salahuddin, R. B. Wilson, J. Gorchon, J. Bokor, and U. Atxitia, Unifying femtosecond and picosecond single-pulse magnetic switching in Gd-Fe-Co, Phys. Rev. B **103**, 104422 (2021).

[12] Y. Xu and S. Mangin, Magnetization manipulation using ultrashort light pulses, J. Magn. Magn. Mater. **564**, 170169 (2022).

[13] J. H. Mentink, J. Hellsvik, D. V. Afanasiev, B. A. Ivanov, A. Kirilyuk, A. V. Kimel, O. Eriksson, M. I. Katsnelson, and T. Rasing, Ultrafast spin dynamics in multisublattice magnets, Phys. Rev. Lett. **108**, 057202 (2012).

[14] A. J. Schellekens and B. Koopmans, Microscopic model for ultrafast magnetization dynamics of multisublattice magnets, Phys. Rev. B **87**, 020407(R) (2013).

[15] N. Bergeard, V. López-Flores, V. Halte, M. Hehn, C. Stamm, N. Pontius, E. Beaurepaire, and C. Boeglin, Ultrafast angular momentum transfer in multisublattice ferrimagnets, Nat. Commun. **5**, 3466 (2014).

[16] V. N. Gridnev, Ultrafast heating-induced magnetization switching in ferrimagnets, J. Phys.: Condens. Matter **28**, 476007 (2016).

[17] A. M. Kalashnikova and V. I. Kozub, Exchange scattering as the driving force for ultrafast all-optical and bias-controlled reversal in ferrimagnetic metallic structures, Phys. Rev. B **93**, 054424 (2016).

[18] S. Wang, C. Wei, Y. Feng, H. Cao, W. Li, Y. Cao, B.-O. Guan, A. Tsukamoto, A. Kirilyuk, A. V. Kimel, and X. Li, Dual-shot dynamics and ultimate frequency of all-optical magnetic recording on GdFeCo, Light: Sci. Appl. **10**, 8 (2021).

[19] F. Steinbach, N. Stetzuhn, D. Engel, U. Atxitia, C. von Korff Schmising, and S. Eisebitt, Accelerating double pulse all-optical write/erase cycles in metallic ferrimagnets, Appl. Phys. Lett. **120**, 112406 (2022).

[20] J. Wei, B. Zhang, M. Hehn, W. Zhang, G. Malinowski, Y. Xu, W. Zhao, and S. Mangin, All-optical helicity-independent switching state diagram in Gd-Fe-Co alloys, Phys. Rev. Appl. **15**, 054065 (2021).

[21] Y. Xu, M. Deb, G. Malinowski, M. Hehn, W. Zhao, and S. Mangin, Ultrafast magnetization manipulation using single femtosecond light and hot-electron pulses, Adv. Mater. **29**, 1703474 (2017).

[22] M. Beens, M. L. M. Lalieu, A. J. M. Deenen, R. A. Duine, and B. Koopmans, Comparing all-optical switching in synthetic-ferrimagnetic multilayers and alloys, Phys. Rev. B **100**, 220409(R) (2019).

[23] C. S. Davies, J. H. Mentink, A. V. Kimel, T. Rasing, and A. Kirilyuk, Helicity-independent all-optical switching of magnetization in ferrimagnetic alloys, J. Magn. Magn. Mater. **563**, 169851 (2022).

[24] M. L. M. Lalieu, M. J. G. Peeters, S. R. R. Haenen, R. Lavrijsen, and B. Koopmans, Deterministic all-optical switching of synthetic ferrimagnets using single femtosecond laser pulses, Phys. Rev. B **96**, 220411(R) (2017).

[25] U. Atxitia, T. A. Ostler, R. W. Chantrell, and O. Chubykalo-Fesenko, Optimal electron, phonon, and magnetic characteristics for low energy thermally induced magnetization switching, Appl. Phys. Lett. **107**, 192402 (2015).

[26] W. Zhang, J. Hohlfeld, T. X. Huang, J.-X. Lin, M. Hehn, Y. Le Guen, J. Compton-Stewart, G. Malinowski, W. S. Zhao, and S. Mangin, Criteria to observe single-shot all-optical switching in Gd-based ferrimagnetic alloys, arXiv:2311.18359.

[27] A. Hassdenteufel, J. Schmidt, C. Schubert, B. Hebler, M. Helm, M. Albrecht, and R. Bratschitsch, Low-remanence criterion for helicity-dependent all-optical magnetic switching in ferrimagnets, Phys. Rev. B **91**, 104431 (2015).

[28] See Supplemental Material at http://link.aps.org/supplemental/10.1103/PhysRevB.108.L220403 for the following: (i) longitudinal magneto-optic Kerr effect hysteresis loops of in-plane magnetized Gd_xCo_{100-x} (t) films with various Gd concentration x and thickness t values. (ii) Out-of-plane magnetic field-dependent magnetization measurements of in-plane magnetized Gd_xCo_{100-x} films. (iii) Magneto-optic domain imaging of in-plane magnetized Gd_xCo_{100-x} films. (iv) Reversed domain diameter versus laser pump pulse energy. (v) Endurance test on in-plane magnetized Gd_xCo_{100-x} films. (vi) Single pulse all-optical helicity-independent switching performed at the magnetic domain wall and two orthogonal in-plane directions. (vii) Pump pulse energy-dependent optical switching measurements of in-plane magnetized Gd_5Co_{95} and $Gd_{30}Co_{70}$ films. (viii) Comparison of the demagnetization threshold and Curie temperature. (ix) Calculation of the absorption profile of GdCo with various sample thicknesses. (x) Definition of the characteristic time of T1 and T2. The Supplemental Material also contains Refs. [6,8,11,30,34–36,39,48,49].

[29] Q. Remy, J. Hohlfeld, M. Verges, Y. Le Guen, J. Gorchon, G. Malinowski, S. Mangin, and M. Hehn, Accelerating ultrafast magnetization reversal by non-local spin transfer, Nat. Commun. **14**, 445 (2023).

[30] M. H. Kryder, E. C. Gage, T. W. McDaniel, W. A. Challener, R. E. Rottmayer, G. Ju, Y.-T. Hsia, and M. F. Erden, Heat assisted magnetic recording, Proc. IEEE **96**, 1810 (2008).

[31] D. O. Ignatyeva, P. O. Kapralov, K. H. Prabhakara, H. Yoshikawa, A. Tsukamoto, and V. I. Belotelov, Magnetization Switching in the GdFeCo films with in-plane anisotropy via femtosecond laser pulses, Molecules **26**, 6406 (2021).

[32] X. Fan and X. Lin, Thermal impact on ultrafast helicity independent all-optical switching of Gd_xCo_{100-x}, J. Phys.: Conf. Ser. **2230**, 012025 (2022).

[33] J. Barker, U. Atxitia, T. A. Ostler, O. Hovorka, O. Chubykalo-Fesenko, and R. W. Chantrell, Two-magnon bound state causes ultrafast thermally induced magnetisation switching, Sci. Rep. **3**, 3262 (2013).

[34] A. R. Khorsand, M. Savoini, A. Kirilyuk, and T. Rasing, Optical excitation of thin magnetic layers in multilayer structures, Nat. Mater. **13**, 101 (2014).

[35] Y. Xu, M. Hehn, W. Zhao, X. Lin, G. Malinowski, and S. Mangin, From single to multiple pulse all-optical switching in GdFeCo thin films, Phys. Rev. B **100**, 064424 (2019).

[36] F. Jakobs and U. Atxitia, Universal criteria for single femtosecond pulse ultrafast magnetization switching in ferrimagnets, Phys. Rev. Lett. **129**, 037203 (2022).

[37] J. Wang, T. Seki, Y.-C. Lau, Y. K. Takahashi, and K. Takanashi, Origin of magnetic anisotropy, role of induced magnetic moment, and all-optical magnetization switching for $Co_{100-x}Gd_x$/Pt multilayers, APL Mater. **9**, 061110 (2021).

[38] M. Verges, W. Zhang, Q. Remy, Y. Le-Guen, J. Gorchon, G. Malinowski, S. Mangin, M. Hehn, and J. Hohlfeld, Extending the scope and understanding of all-optical magnetization switching in Gd-based alloys by controlling the underlying temperature transients, arXiv:2309.14797.

[39] N. H. Duc and D. Givord, Exchange interactions in amorphous Gd Co alloys, J. Magn. Magn. Mater. **157**, 169 (1996).

[40] P. Hansen, C. Clausen, G. Much, M. Rosenkranz, and K. Witter, Magnetic and magneto-optical properties of rare-earth transition-metal alloys containing Gd, Tb, Fe, Co, J. Appl. Phys. **66**, 756 (1989).

[41] B. Koopmans, G. Malinowski, F. Dalla Longa, D. Steiauf, M. Fähnle, T. Roth, M. Cinchetti, and M. Aeschlimann, Explaining the paradoxical diversity of ultrafast laser-induced demagnetization, Nat. Mater. **9**, 259 (2010).

[42] T. Ferté, M. Beens, G. Malinowski, K. Holldack, R. Abrudan, F. Radu, T. Kachel, M. Hehn, C. Boeglin, B. Koopmans, and N. Bergeard, Laser induced ultrafast Gd 4f spin dynamics in $Co_{100-x}Gd_x$ alloys by means of time-resolved XMCD, Eur. Phys. J.: Spec. Top. **232**, 2213 (2023).

[43] S. R. Tauchert, M. Volkov, D. Ehberger, D. Kazenwadel, M. Evers, H. Lange, A. Donges, A. Book, W. Kreuzpaintner, U. Nowak, and P. Baum, Polarized phonons carry angular momentum in ultrafast demagnetization, Nature (London) **602**, 73 (2022).

[44] G. Malinowski, F. Dalla Longa, J. H. H. Rietjens, P. V. Paluskar, R. Huijink, H. J. M. Swagten, and B. Koopmans, Control of speed and efficiency of ultrafast demagnetization by direct transfer of spin angular momentum, Nat. Phys. **4**, 855 (2008).

[45] G.-M. Choi, B.-C. Min, K.-J. Lee, and D. G. Cahill, Spin current generated by thermally driven ultrafast demagnetization, Nat. Commun. **5**, 4334 (2014).

[46] B. Liu, H. Xiao, and M. Weinelt, Microscopic insights to spin transport–driven ultrafast magnetization dynamics in a Gd/Fe bilayer, Sci. Adv. **9**, eade0286 (2023).

[47] M. Hennecke, D. Schick, T. Sidiropoulos, F. Willems, A. Heilmann, M. Bock, L. Ehrentraut, D. Engel, P. Hessing, B. Pfau, M. Schmidbauer, A. Furchner, M. Schnuerer, C. von Korff Schmising, and S. Eisebitt, Ultrafast element- and depth-resolved magnetization dynamics probed by transverse magneto-optical Kerr effect spectroscopy in the soft x-ray range, Phys. Rev. Res. **4**, L022062 (2022).

[48] Q. Remy, J. Igarashi, S. Iihama, G. Malinowski, M. Hehn, J. Gorchon, J. Hohlfeld, S. Fukami, H. Ohno, and S. Mangin, Energy efficient control of ultrafast spin current to induce single femtosecond pulse switching of a ferromagnet, Adv. Sci. **7**, 2001996 (2020).

[49] J. Igarashi, Q. Remy, S. Iihama, G. Malinowski, M. Hehn, J. Gorchon, J. Hohlfeld, S. Fukami, H. Ohno, and S. Mangin, Engineering single-shot all-optical switching of ferromagnetic materials, Nano Lett. **20**, 8654 (2020).